Giant Magnetoresistance of the Electrodeposited FeCoCu/Cu Multilayers: Metal Oxide Formation with NaOH in the Electrolyte

A. Tekgül[a,*], T. Şahin[b,c], H. Köçkar[b] and M. Alper[a]

[a] *Uludag University, Physics Department, Science and Literature Faculty, TR-16059, Bursa, Turkey*
[b] *Balıkesir University, Physics Department, Science and Literature Faculty, TR-10145, Balıkesir, Turkey*
[c] *Electrical and Electronics Engineering, Gelisim University, TR-34100, İstanbul, Turkey*

Received: 08.01.2023 & Accepted: 19.01.2023

Doi: 10.12693/APhysPolA.143.262 *e-mail: atakantekgul@gmail.com

FeCo(CoO)Cu/Cu multilayers were prepared from the electrolytes containing various amounts of NaOH by the electrochemical deposition technique. The current density decreases with the increasing molarity of NaOH in the electrolyte. Therefore, the magnetic layers deposit more slowly on the Cu layers. This may cause the oxidation of the magnetic elements. The structural analysis was performed by the X-ray diffraction technique, and the refined patterns exhibit that the multilayers have a face-centered-cubic crystal structure (Fm-3m space group). The magnetic hysteresis curves were measured by the vibrational sample magnetometers at room temperature. The saturation magnetization of the multilayers was found to be 53.02, 24.83, and 24.26 A m^2/kg as a function of the NaOH amount in the electrolyte. Magnetoresistance values were measured and observed to change from 16 to 2.5% when the NaOH amount increased from 0.01 to 0.02 M in the electrolyte, and the 7% anisotropic magnetoresistance was obtained for 0.01 M NaOH. The results indicate that the NaOH may cause the occurrence of metal oxide in the magnetic layers for the multilayers produced from the electrolyte with 0.02 and 0.04 M NaOH, and this metal oxide is CoO since its crystal structure is similar to the Co, Fe, and Cu, and also, the magnetization drastically decreases with increasing NaOH amount.

topics: electrochemical deposition, multilayer, sodium hydroxyl, magnetoresistance

1. Introduction

Nowadays, high-technological applications such as solar cell batteries, semiconductor devices, magnetic recording, magnetic sensors, etc., play an essential role in human life [1–3]. These applications begin to miniaturize from bulk to micro- or nano-size with the new technology. The main reason for this approach is that the bulk materials cause high Eddy current loss and degrade the quality factor of the applications [4]. Here, electrical resistivity and magnetic hysteresis lead to this current loss. Both the reduction of the electrical resistivity and the narrow hysteresis curve minimizes the Eddy current loss, and therefore, magnetic thin films are a candidate for high-technological applications. Similar to the coil core, the multilayered form of thin films, which consist of two ferromagnetic layers (FM) divided by a non-magnetic layer (NM), is the best option to reduce the loss. The multilayered (or granular multilayer) thin films have an anisotropy field and high saturation magnetization, and therefore, they are preferred for magnetic devices and sensors. These multilayers exhibit giant magnetoresistance (GMR) due to the layered form [5, 6]. The GMR is a resistivity change under the application of a magnetic field, and due to the spin-dependent scattering, the electron spins play an important role that passes through a layered form which consists of two ferromagnetic layers separated by a non-magnetic layer. When the magnetic orientations of the ferromagnetic layers are parallel to each other under a magnetic field, the resistivity (R_P) for parallel configuration is lower than the resistivity (R_{AP}) for the antiparallel configuration under a zero magnetic field. This effect has been discovered independently by both Peter Grünberg and Albert Fert in Fe/Cr/Fe multilayered structure, who separately, together with co-workers, have used molecular beam epitaxy to grow this multilayer [7, 8]. The molecular beam epitaxy is a highly efficient technique for producing thin films and multilayers, and the layer surface of the multilayers has a fairly smooth geometry. Alper et al. [9] have observed the GMR effect in Cu/CoNiCu super-lattice produced by the electrochemical deposition. The electrochemical deposition technique is an alternative way to produce the multilayer, and the layer surface is non-uniform.

The diffusive scattering of electrons due to interface roughness has to be taken into account [8, 10]. The non-uniform surface causes the interface scattering between ferromagnetic and non-magnetic layers, and therefore, the resistivity begins to increase, leading to an increase in the GMR value. Camley and Barnaś [11] showed that the number of layers and the ratio of mean free path to thickness have increased the magnetoresistance effect significantly. Also, electrochemical deposition is low-cost, easy to employ without a vacuum, and allows the production of the desired geometry. To obtain the high GMR, the iron triad (Fe, Co, Ni) and Cu, Cr, Ag are generally used in the electrochemical deposition for the ferromagnetic and non-magnetic layers, respectively [12–18].

During the production of the multilayer, their structural, electrical, mechanical, and magnetic properties can be controlled by many parameters, such as the ferromagnetic/non-magnetic layer thickness, the ion concentrations, the electrolyte pH, the electrochemical bath, and the cathode potentials. The single and dual baths techniques are used to produce the multilayer formation. There are some advantages and disadvantages of these baths. The separation of the layers is clearer in the dual bath, but the contamination and oxidation risk is higher than in the single bath during the transfer from one bath to another bath (or baths). In the single bath, the electrochemical deposition potentials determine the deposited metal or metals, and the dissolution or co-deposition can occur during the transition between the deposition potentials [9, 19, 20]. The higher potentials cause the dissolution, and the selection of the potentials can be optimized. In the co-deposition, the nobility of the metals plays a crucial role, and hence, the noble metal ion concentrations are lower than that of less noble metals in the electrolyte. On account of this, the bath formulations directly affect the quality of the multilayer since the electrolyte preparation is the main part of the electrochemical deposition, and its temperature, pH level, and regulator agents are the adjusting mechanism of the quality of the multilayer.

Especially for Fe-containing multilayers, the main problem is the presence of Fe^{2+} ions in the electrochemical deposition bath. Since the occurrence of Fe precipitation begins before the deposition process, the Fe ion amount in the ferromagnetic layers drastically decreases in the final multilayer. The multilayers containing Fe are mostly prepared from sulphate, nitrate, and citrate solutions. These solutions include hydroxide ions. During the preparation of the electrolyte, the regulator agents such as boric acid (H_3BO_3), citric acid ($H_3C_6H_5O_7.H_2O$), and L-ascorbic acid ($C_6H_8O_6$) are used to control the stability. Although the boric acid is added to hinder the hydroxide ion deposition on the film surface, it causes a small amount of Fe deposition [21]. Zalka et al. [15] presented a study about the bath type in 2019. They produced the CoFe/Cu multilayer series from sulphamate, sulphate, chloride, and citrate baths containing the boric acid to increase the Fe ion amount in the layers. They found that the Fe deposition is relatively low while the molarity of the Fe ions increases. On the other hand, when the thin films are produced from the electrolyte containing citric acid, a large of amount Fe content and the lowest current efficiency are observed, and hydroxide ion deposition occurs on the surface. But, the Fe^{2+} ions begin to transform into more stable Fe^{3+} ions because of the citric acid. L-ascorbic acid provides the protection of metal ions from oxidation. However, hydroxide ion deposition is observed when the multilayer is deposited from the electrolyte containing L-ascorbic acid, and a large amount of Fe ions can be deposited on the surface of the layers. In our previous study [22], we used the L-ascorbic acid to regulate the electrolyte and produced the FeCoCu/Cu granular multilayers, but the results have shown that the increase in L-ascorbic acid molarity leads to the increase in the deposited Fe amount and also, the decrease in the magnetoresistance value. Consequently, these regulators (citric acid and L-ascorbic acid) allow the increase in the Fe amount of the ferromagnetic layers, but their disadvantages cause abnormal deposition. In the previous work of our group [23], the pH value is adjusted from 3.70 to 2.70 with NaOH content, and a large amount of the Fe is found at a low pH value.

In the present study, we used NaOH to regulate the electrolyte, and the pH value of the electrolyte is held constant at 2.80. The NaOH is used in certain amounts such as 0.01, 0.02, and 0.04 M. For 0.01 M NaOH, the properties of the multilayer are similar to that in the literature. When the amount of the NaOH is increased to 0.02 M in the electrolyte, a high amount of the NaOH causes the occurrence of metal oxide as the deposited multilayers from the electrolyte containing the L-ascorbic acid. Hence, in our composition, the magnetic layer contains metal oxide sites in the FeCoCu/Cu multilayer. The structural and magnetic results show that the multilayer is the FeCo(CoO)Cu/Cu, which is produced from the electrolyte with 0.02 and 0.04 M NaOH. Here, iron and copper oxides have a rhombohedral and monoclinic structure [24, 25], and there are no peaks related to this crystal structure in the X-ray diffraction patterns. Also, the decrease in magnetization could be related to the magnetic metal ions. Cobalt oxides are interesting due to their unique physical and chemical properties, which make them promising materials for application in rechargeable Li-ion batteries [26], catalysis [27], gas sensing [28], and others. Consequently, the multilayers produced from the electrolyte with 0.02 and 0.04 M NaOH have the CoO sites and also exhibit the MR property. Our multilayers are a candidate material for these applications. Therefore, electrochemical, structural, magnetic, and magnetoresistance behaviors of the FeCoCu/Cu multilayers containing CoO were analyzed in detail.

2. Experimental

2.1. Electrolytes for preparing the FeCo(CoO)Cu/Cu multilayers

For multilayer deposition, two-pulse plating from a single bath was applied on a substrate. Main electrolyte includes $CoSO_4$ $7H_2O$, $FeSO_4$ $7H_2O$, and $CuSO_4$ $4H_2O$. According to the inductively coupled plasma-mass spectrometer, 0.470 M Co, 0.100 M Fe, and 0.030 M Cu were found in the electrolyte. Three different electrolytes were prepared with the additive substances, H_3BO_3 and NaOH. To investigate the NaOH effect, 0.01, 0.02, and 0.04 M NaOH were added to the main electrolyte separately, and then a proper amount of the H_3BO_3 was used to adjust the pH at 2.80 ± 0.02. The relative Fe^{2+} ion concentration $c_{ion,Fe}$ in the bath was defined by the ionic ratio $Fe^{2+}/[Fe^{2+}+Co^{2+}]$, and it was found to be 17.5 mol%. The deposition potentials were determined from the cyclic voltammetry technique. The proper values for non-magnetic and ferromagnetic layers were found at -0.3 V and -1.6 V versus standard calomel electrode, respectively.

2.2. Production of the FeCo(CoO)Cu/Cu multilayers

The FeCo(CoO)Cu/Cu multilayers were produced on polycrystalline titanium sheet substrates by electrochemical deposition. The multilayers were deposited in a cylindrical cell with three electrodes using a potentiostat/galvanostat (EG&G Princeton Applied Research Model 362) controlled by a personal computer. The distance between the cathode and anode electrodes is about 9.4 cm. The bilayer numbers were chosen so that the nominal thickness is about 3 μm in the rectangular area of 2.9 cm^2 and the layer thickness was held constant at 6/3 nm (ferromagnetic/non-magnetic). Upon completion of growth, the films were peeled off their substrates mechanically. The charge flowing through the system was recorded during the potentiostatic pulse. Then, the nominal thickness can be calculated from Faraday's law using

$$d = \frac{Q\,\eta}{z\,F\,A}\,\frac{M}{\rho}. \tag{1}$$

Here, Q, z, F, and A are the quantity of deposited metals, valance electrons of its metal ion, Faraday constant, and surface area, respectively; M is the molar weight; ρ is the density of its metal ion; $\eta$is a current efficiency.

2.3. Characterizations of the FeCo(CoO)Cu/Cu multilayers

The morphological and elemental analysis of the produced FeCo(CoO)Cu/Cu multilayers was determined by scanning electron microscopy (SEM) with energy dispersive X-ray spectrometry (EDX). The structural analysis was performed by the X-ray diffraction (XRD) technique (Philips Analytical XRD PW3040/60 model) with Cu K_α radiation in the range of $2\theta = 30$–$80°$. The obtained XRD spectra were refined using the Rietveld method by the FullProf software. The crystallite size of the multilayers was used with the Scherrer equation [29].

The vibrating sample magnetometer (VSM) (ADE technologies DMS-EV9 Model) was used to determine the magnetic properties of the multilayers in the range of ± 2 T. The magnetic field was applied in parallel and perpendicular directions to the surface of the multilayer. Magnetoresistance (MR) measurements were performed in the range of ± 1 T at room temperature. The Van der Pauw method used the MR change using

$$R[\%] = \frac{R(H) - R_{\min}}{R_{\min}} \times 100 \tag{2}$$

Here, $R(H)$ is the measured electrical resistance value at any magnetic field, and R_{min} is the minimum measured resistance. The magnetic field was applied both parallel and perpendicular to the current flowing in the film plane to measure the longitudinal magnetoresistance (LMR) and transverse magnetoresistances (TMR), respectively. The anisotropic magnetoresistance (AMR) was found with AMR=|LMR-TMR|.

3. Results and discussion

The obtained current density-time transients during the electrochemical deposition are given in Fig. 1. The black, red, and blue lines show the current density-time transients of the multilayer produced from the electrolyte containing 0.01, 0.02, and 0.04 M NaOH, respectively. The high current pulses correspond to the magnetic layers, and the low refer to non-magnetic layers on the cathodic side. On the anodic side, the current pulses arise from a capacitive transient, and these cause the dissolution of the magnetic layers. After the magnetic layer deposits on the cathode, the capacitive transient dissolves some magnetic particles. Therefore, the nominal magnetic layer thickness decreases the expected thickness. Here, Cu is nobler than Co and Fe, and hence some Cu atoms deposit with the magnetic layers. The nominal Cu layer thickness is higher than the expected one. In the figures, the deposition time of the Cu layers is longer than that of the magnetic layers since the total concentration of Co ions in the electrolyte is more than the Cu ions concentration. The current density for both the magnetic layers and non-magnetic layers begins to decrease with the increase in the NaOH amount in the electrolyte, and the addition of the OH ions causes the decrease in the current. Therefore, the deposition time of the layers increases due to the NaOH. In the literature, the maximum current density of the multilayers containing Co, Fe, and Cu for the magnetic layer produced by the electrochemical

TABLE I

Previous studies produced from the various bath compositions.

Current density [m A/cm^2]	Boric acid [M]	Sulfamic acid [M]	Ascorbic acid [M]	Ammonium sulphate [M]	Ammonium chloride [M]	Citric acid [M]	NaOH [M]	pH	Ref.
85.90	Adj.	–	–	–	–	–	0.01	2.8	This work
71.67	Adj.	–	–	–	–	–	0.02	2.8	This work
56.56	Adj.	–	–	–	–	–	0.04	2.8	This work
68.02	0.25	0.01	–	–	–	–	–	2.5	[13]
51.39	0.25	0.01	–	–	–	–	–	2.6	[14]
60.01	0.25	–	0.01	–	–	–	–	2.5	[22]
68.01	0.25	–	0.02	–	–	–	–	2.3	[22]
67.5	0.25	–	0.04	–	–	–	–	2.1	[22]
67.4	0.25	–	0.06	–	–	–	–	2	[22]
57.5	0.25	–	0.08	–	–	–	–	1.95	[22]
51	0.25	–	0.1	–	–	–	–	1.9	[22]
65	0.5	–	–	–	–	–	0.01	3.7, 3.3, 3.0, 2.7	[23]
52.08	0.25	0.01	–	–	–	–	–	2.5	[31]
57.29	0.25	0.01	–	–	–	–	–	2.5	[32]
31.25	0.25	0.25	–	–	–	–	–	3.25	[33]
20.7, 34.5	0.25	0.25	–	0.14	–	–	–	3.6	[34]
20.7, 34.5	0.25	–	–	0.14	–	–	–	2.8	[34]
20.7, 34.5	0.25	–	–	–	0.14	–	–	3.2	[34]
20.7, 34.5	0.25	–	–	–	–	0.2	–	5.6	[34]
65.97	0.25	–	–	–	–	–	–	2.5	[35]
3.7, 4.7, 6.4, 7.2, 9.3	0.5	–	0.006	–	–	–	–	3.5	[36]
69.4	0.5	–	–	–	–	–	–	2.1	[37]

TABLE II

The calculated magnetic and non-magnetic layer thicknesses from the current–time curves.

	Magnetic layer thickness [nm]	Non-magnetic layer thickness [nm]	A/B Eq. (6)	C/D Eq. (7)
0.01 M NaOH	5.8328	3.4460	1.087/2.135	0.647/10.528
0.02 M NaOH	5.8335	3.5305	1.249/1.392	0.549/6.776
0.04 M NaOH	5.8325	3.5713	2.717/0.770	0.636/4.823

deposition is given in Table I. Various regulators have been used to adjust the pH and current flow of the bath. In the present work, the current density in the electrolyte containing 0.01 M NaOH is higher than that in the literature, and it drastically decreases due to the NaOH amount in the electrolyte. The nominal thickness of the layers can be calculated on the basis of Faraday's law (1) from the current–time transients. In this equation, the current efficiency was taken as 100% since hydrogen evolution was negligible for the Co-rich layer deposition [30]. The calculated layer thicknesses are given in Table II (see also [13, 14, 22, 23, 31–37]). The magnetic layer thickness is $\simeq 5.8$ nm, and the dissolving of the layer is almost the same for all electrolytes. On the other hand, the Cu ions deposit more than the dissolving ion amounts with increasing NaOH molarity in the electrolyte.

Figure 2a, 2b, and 2c shows the Rietveld refined XRD pattern of the multilayers produced from the electrolyte, which includes the 0.01, 0.02, and 0.04 M NaOH, respectively. In the figure, the red circle and black line indicate the observed and calculated data and the blue line is the difference between the observed and calculated patterns. The Bragg positions are presented at the bottom of each panel. The crystal structure was found to be a face-centered-cubic (fcc) structure (Fm-$3m$ space group). The χ^2 value of the patterns is 1.11, 4.56, and 2.23. These results show that all multilayers

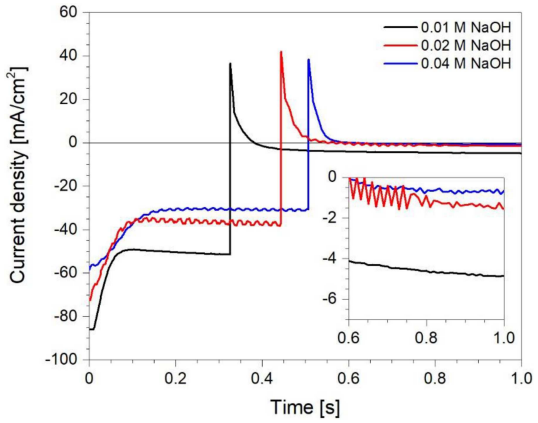

Fig. 1. Recorded current density-time curves of the multilayers during the deposition. Inset figure indicates the deposition curves of the Cu layer.

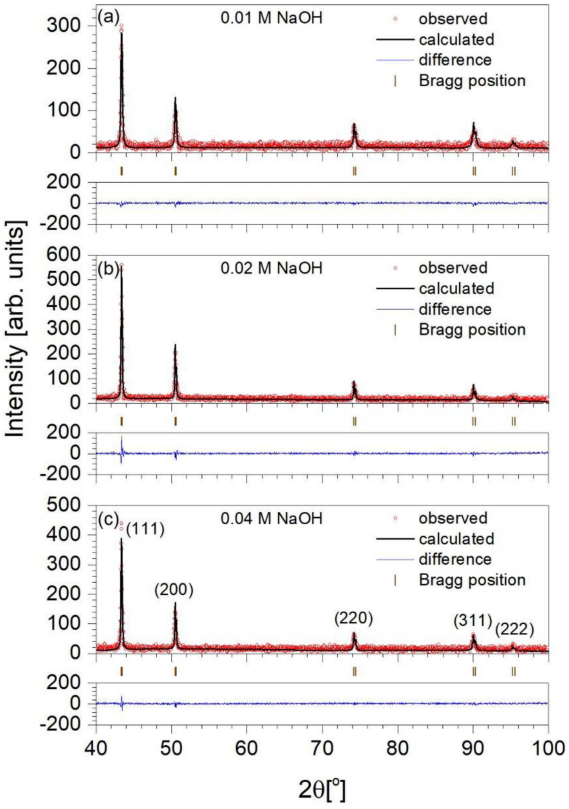

Fig. 2. Refined XRD patterns of the multilayer produced from the electrolyte with (a) 0.01, (b) 0.02, and (c) 0.04 M NaOH.

are polycrystalline, with both magnetic and non-magnetic layers adopting the fcc structure. The peaks of $2\theta = 43°$, $50°$, $74°$, $90°$, and $95°$ were observed at all patterns and are related to (111), (220), (222), (311), and (222) planes, respectively. The lattice parameter is around 0.3612 nm for all patterns, and the small increase occurs in the volume of the unit cell. These confirm the nominal thickness results since the increase in NaOH causes

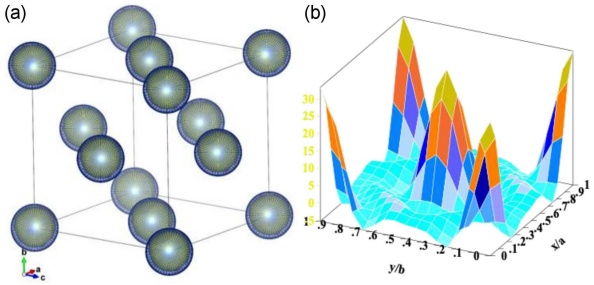

Fig. 3. (a) The crystal structure of the multilayer obtained from the Rietveld refinement and (b) the Fourier map of the unit cell.

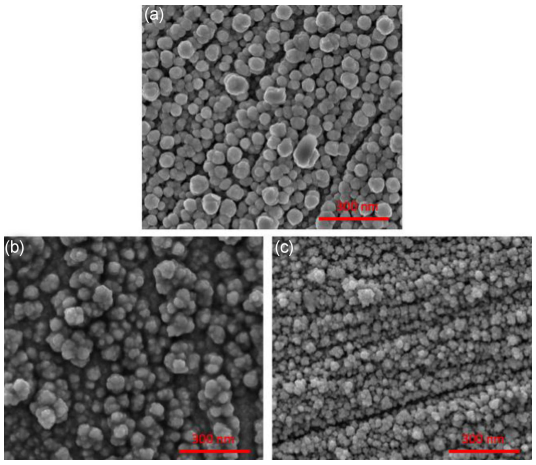

Fig. 4. SEM images of the multilayers produced from the electrolyte with (a) 0.01, (b) 0.02, and (c) 0.04 M NaOH.

the increase in the Cu amount, and the lattice parameter of the Cu is close to these values. We obtained the crystalline size of the multilayers using the Scherrer equation; 33, 30, and 27 nm are found for the multilayers produced from the electrolyte with 0.01, 0.02, and 0.04 M NaOH.

Figure 3 shows the Fm-$3m$ crystal structure of the multilayer obtained from the FullProf software with the Rietveld refinement. The atoms are located at (x, y, z) 3D symmetry, and the calculated Fourier maps show that the electron density is concentrated in the origin and corners of the unit cell.

The scanning electron microscopy images of the multilayers are given in Fig. 4a–c. The measurements are performed at 20 keV at $4k$ magnification. The particle geometry of the multilayer produced from the electrolyte with 0.01 M NaOH has a nearly spherical form, and the particle distribution is homogeneous. When the NaOH amount is 0.02 M in the electrolyte, the particles grow like cauliflower in some areas, and the size of the particle is smaller than that in the initial multilayer. The cauliflower form of the multilayer produced from the electrolyte with 0.04 M NaOH is smaller than that of the multilayer seen in Fig. 4b.

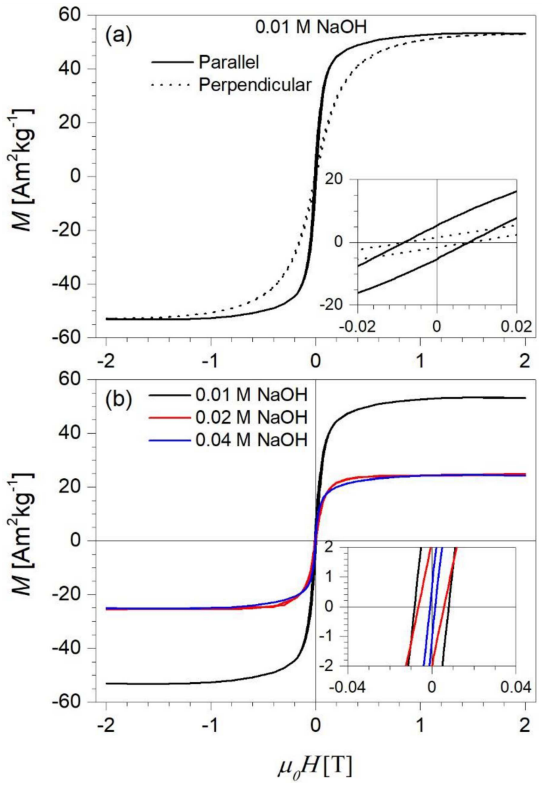

Fig. 5. (a) The parallel and perpendicular hysteresis curves of the multilayer produced from the electrolyte with 0.01 M NaOH and (b) the parallel hysteresis curves of all multilayers.

Figure 5a–b shows the field-dependent magnetization curves of the multilayers at room temperature in the range of a ±2 T magnetic field. The parallel and perpendicular hysteresis loops of the multilayer produced from the electrolyte with 0.01 M NaOH are presented in Fig. 5a. The curves appear to be rapidly saturated in very low fields due to the low thermal interactions at room temperature. The difference between parallel and perpendicular curves is small, and this shows that the uniaxial anisotropy is low and the multilayer exhibits nearly bulk property. The coercivity of the multilayer is the same in both the parallel and perpendicular curves, i.e., 8 mT. In Fig. 5b, the variation of the hysteresis curves is presented due to the NaOH amount in the electrolyte. The saturation magnetization of the multilayers is 53.02, 24.83, and 24.26 A m^2/kg, respectively. In our previous work [22], we studied the L-ascorbic acid effect on the FeCoCu/Cu magnetic multilayer granular films and observed the layer oxidized due to the OH ion. Similarly, the Cu ions are reduced by the hydroxide, as seen by

$$Cu^{2+} + 2\,OH^- \rightarrow Cu(OH)_2 \qquad (3)$$

When the magnetic ions begin to deposit on the surface, they encounter the $Cu(OH)_2$ as explained in [38, 39], and the following reactions could occur on the layer surface

$$\begin{aligned} &2Fe^{2+} + 3Cu(OH)_2 \rightarrow 2Fe^{2+} + 3CuO + 3H_2O \rightarrow \\ &\quad \rightarrow Fe_2O_3 + 3Cu^{2+} + 3H_2O \\ &Co^{2+} + Cu(OH)_2 \rightarrow Co^{2+} + CuO + H_2O \rightarrow \\ &\quad \rightarrow CoO + Cu^{2+} + H_2O \end{aligned} \qquad (4)$$

These reactions show that magnetic layers partially transform the mixed layers containing the metal and metal–oxide during the deposition. The Fe_2O_3 and the CoO are antiferromagnetic at room temperature [40, 41]. On the other hand, the CoO and Fe_2O_3 are an fcc and rhombohedral crystal structure [24, 42] and our XRD results confirm that the crystal structure of the multilayers is fcc. Hence, the peaks of CoO overlap with the peaks of the multilayers. The drastic decrease in magnetization confirms these reactions. Furthermore, the ferromagnetic layers have antiferromagnetic (AFM) sites, and the multilayers consist of periodic FM(AFM)/NM layers. Therefore, both FM coupling and AFM coupling occur between the magnetic layers. The magnetization decreases from 53.02 to 24.26 A m^2/kg due to the changes in the NaOH amount since the AFM sites increase when the amount of NaOH increases from 0.01 to 0.02 M in the electrolyte. The change of the coercivity was found to be 7.9, 5.9, and 1.6 mT under a 2 T magnetic field as a function of the NaOH amount in the electrolyte. The coercivity value decreases with the particle size in the study of Zhang et al. [41] (they produced the CoO nanoparticles). In our study, the particle size

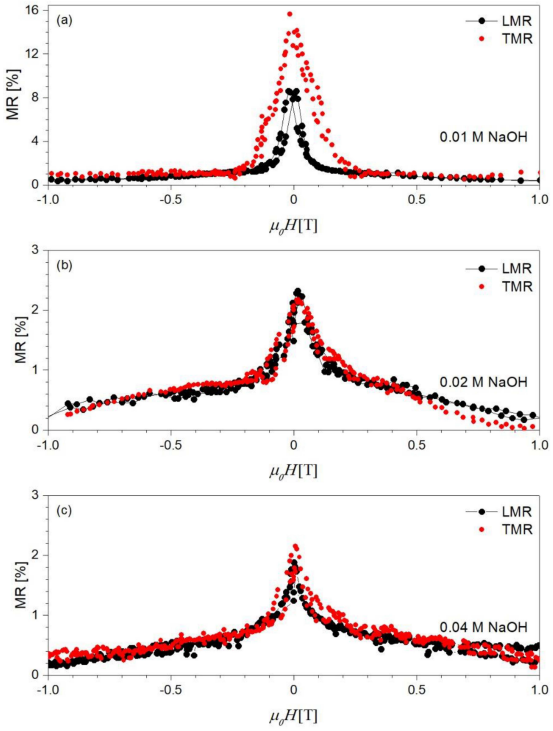

Fig. 6. MR change of the multilayers produced from the electrolyte with (a) 0.01, (b) 0.02, and (c) 0.04 M NaOH.

is bigger than that of Zhang et al. [41], and also, our multilayers include the Co particles. Consequently, the coercivity value decreases due to the CoO and Fe_2O_3 in the present work. The electrolyte has rich-cobalt ions, and hence, the contribution of the CoO is more than that of the Fe_2O_3 in the coercivity change.

Figure 6a–c shows both longitudinal magnetoresistance (LMR) and transverse magnetoresistance (TMR) change in the range of ±1 T magnetic field. For the multilayer produced from the electrolyte with 0.01 M NaOH in Fig. 6a, the LMR and TMR values were found to be 9% and 16%, respectively. The LMR has a wide full-width half-maximum (FWHM), and the MR change occurs in the range of 0–0.2 T. On the other hand, the TMR curve can reach a maximum at a low magnetic field, and splitting occurs at a maximum MR value. The hysteresis of this multilayer causes the splitting because of its coercivity value. As one can see, there is a 7% difference between the LMR and the TMR curves (anisotropic magnetoresistance AMR = |LMR − TMR|). When the NaOH amount increases from 0.01 to 0.02 M and then to 0.04 M, the occurrence of the CoO and Fe_2O_3 partially prevents the interaction of the magnetic layers, and hence, the LMR and TMR curves of the multilayers are close to each other. But, the magnetic layers with metal-oxide decrease the saturation magnetization, and as a result of this decrease, the MR value is observed around 2.5%. The AMR is nearly zero for the multilayers produced from the electrolyte with 0.02 and 0.04 M NaOH.

4. Conclusions

The FeCoCu/Cu multilayers were deposited from the electrolyte with 0.01, 0.02, and 0.04 M NaOH by the electrochemical deposition technique. The effect of NaOH was investigated on the electrochemical, structural, magnetic, and magnetoresistance properties of the multilayers. The previous studies are produced on the various baths with different ingredients by the electrochemical deposition, and the NaOH effect on the electrochemically deposited multilayers is not much investigated. The current–time curves were recorded during the deposition process. The maximum peak of current density decreases with the NaOH amount in the electrolyte, and hence, this causes an increase in the time of both magnetic and non-magnetic layer deposition. The slow deposition of the magnetic layer may cause oxidation in the magnetic elements and can create the formation of CoO zones. The X-ray diffraction technique was used to determine the structure of the multilayers. The peaks of $2\theta = 43°$, 50°, 74°, 90°, and 95° were observed and are related to (111), (220), (222), (311), and (222) planes, respectively. The Rietveld refinement was applied to the patterns, and the multilayers have an fcc structure at room temperature. The calculated lattice parameters are close to each other, and the crystalline size is found to be 33, 30, and 27 nm using the Scherrer equation. In the parallel and perpendicular hysteresis loops of the multilayer, the saturation magnetization of the multilayers is 53.02, 24.83, and 24.26 A m^2/kg as a function of the NaOH amount in the electrolyte. This drastic decrease is due to the occurrence of the antiferromagnetic CoO in the magnetic layers. In the MR measurements, the decrease is observed, as seen in the saturation magnetization, but the crystal anisotropy and the anisotropic magnetoresistance decrease with the NaOH amount in the electrolyte. In appearance, the CoO sites prevent the strong interaction of the layers containing Co since, generally, the Co–Co interaction causes anisotropy in the magnetic layers. Therefore, the decrease in the magnetic interaction increases the possibility of movement of magnetic moments due to the direction of the magnetic field. Consequently, using the NaOH ingredient conduces the transition metal oxide in the magnetic layers, and therefore, the multilayer can be named the FeCo(CoO)Cu/Cu. Our multilayers are promising candidate materials for Li-ion batteries, gas sensing, and catalysis applications.

Acknowledgments

This paper was financially supported by Balikesir University under Grant No. BAP 2012/33. The authors would like to thank the Scientific and Technical Research Council of Turkey (TUBITAK) under Grant No. TBAG-1771 for the electrodeposition system. The authors are grateful to Dr. H. Guler for the XRD measurement, Balikesir University, Turkey, and thank the UNAM at Bilkent University, Turkey, for SEM and EDX measurements. The authors thank the State Planning Organization, Turkey, under Grant No. 2005K120170 for the VSM system and Balikesir University BAP under Grant No. 2001/02 and 2005/18 for the MR system.

All authors contributed to the study's conception and design. Material preparation, data collection and analysis were performed by Turgut Şahin, Atakan Tekgül, and Hakan Köçkar. The first draft of the manuscript was written by Atakan Tekgül, and all authors commented on previous versions of the manuscript. All authors read and approved the final manuscript.

References

[1] R.L. White, *IEEE Trans. Magn.* **30**, 346 (1994).

[2] H. van den Berg, U. Hartmann, R. Coehoorn, M. Gijs, P. Grünberg, T. Rasing, K. Röll, *Magnetic Multilayers and Giant Magnetoresistance: Fundamentals and Industrial Applications*, Springer, Berlin 2013.

[3] C. Reig, S. Cardoso, S. Mukhopadhyay, *Giant Magnetoresistance (GMR) Sensors: From Basis to State-of-the-Art Applications*, Springer, Berlin 2013.

[4] J.M. Daughton, *J. Magn. Magn. Mater.* **192**, 334 (1999).

[5] J. Daughton, J. Brown, E. Chen, R. Beech, A. Pohm, W. Kude, *IEEE Trans. Magn.* **30**, 4608 (1994).

[6] A. Tekgül, M. Alper, H. Kockar, H. Kuru, *J. Mater. Sci.* **52**, 3368 (2017).

[7] P. Grünberg, R. Schreiber, Y. Pang, M.B. Brodsky, H. Sowers, *Phys. Rev. Lett.* **57**, 2442 (1986).

[8] M.N. Baibich, J.M. Broto, A. Fert, F.N. Van Dau, F. Petroff, P. Etienne, G. Creuzet, A. Friederich, J. Chazelas, *Phys Rev Lett* **61**, 2472 (1988).

[9] M. Alper, K. Attenborough, R. Hart, S.J. Lane, D.S. Lashmore, C. Younes, W. Schwarzacher, *Appl. Phys. Lett.* **63**, 2144 (1993).

[10] G. Binasch, P. Grünberg, F. Saurenbach, W. Zinn, *Phys. Rev. B* **39**, 4828 (1989).

[11] R.E. Camley, J. Barnaś, *Phys. Rev. Lett.* **63**, 664 (1989).

[12] A. Tekgül, H. Kockar, H. Kuru, M. Alper, C.G. ÜnlÜ, *J. Electron. Mater.* **47** 1896 (2018).

[13] A. Tekgül, H. Kockar, M. Alper, *J. Supercond. Nov. Magn.* **31**, 2195 (2018).

[14] A. Tekgül, H. Köçkar, M. Alper, *Thin Solid Films* **673**, 7 (2019).

[15] D. Zalka, L. Péter, M. El-Tahawy, J. Gubicza, G. Molnár, I. Bakonyi, *J. Electrochem. Soc.* **166**, D923 (2019).

[16] M. Spilka, R. Babilas, W. Ratuszek, J. Kowalska, K. Matus, *Arch. Metall. Mater.* **63**, 2067 (2018).

[17] S. Agarwal, D. Pohl, A.K. Patra, K. Nielsch, M.S. Khatri, *Mater. Chem. Phys.* **230**, 231 (2019).

[18] S. Saher, M. Khaleeq-ur-Rahman, F. Arshad, S. Riaz, S. Naseem, *IEEE Trans. Magn* **54**, 1 (2018).

[19] A.M. Białostocka, U. Klekotka, B. Kalska-Szostko, *Sci. Rep.* **10**, 1029 (2020).

[20] H. Kuru, H. Kockar, M. Alper, *J. Magn. Magn. Mater.* **444**, 132 (2017).

[21] V.C. Kieling, *Surf. Coat. Technol.* **96**, 135 (1997).

[22] T. Şahin, A. Tekgül, H. Köçkar, M. Alper, *Thin Solid Films* **709**, 138180 (2020).

[23] T. Sahin, H. Kockar, M. Alper, *J. Supercond. Nov. Magn.* **26**, 825 (2013).

[24] E. Kendir, A. Tekgül, İ. Küçük, Ş. Yaltkaya, *J. Electron. Mater.* **49**, 798 (2020).

[25] J.B. Forsyth, S. Hull, *J. Phys. Condensed Matter* **3**, 5257 (1991).

[26] J.-M. Chen, C.-T. Hsieh, H.-W. Huang, Y.-H. Huang, H.-H. Lin, M.-H. Liu, S.-C. Liao, H.-C. Shih, US Patent US7323218B2: Synthesis of Composite Nanofibers for Applications in Lithium Batteries, 2008.

[27] J. Yang, H. Liu, W.N. Martens, R.L. Frost, *J. Phys. Chem. C* **114**, 111 (2010).

[28] D.Y. Kim, H. Kang, N.-J. Choi, K.H. Park, H.-K. Lee, *Sens. Actuators B* **248**, 987 (2017).

[29] P. Scherrer, *Bestimmung der Größe und der inneren Struktur von Kolloidteilchen mittels Röntgenstrahlen* in: *Kolloidchemie Ein Lehrbuch*, Ed. R. Zsigmondy, Göttinger Nachrichten Gesell., 1918, p. 98 (in German).

[30] I. Bakonyi, L. Peter, *Prog. Mater. Sci.* **55**, 107 (2010).

[31] A. Tekgül, M. Alper, H. Kockar, *J. Mater. Sci. Mater. Electron.* **27**, 10059 (2016).

[32] A. Tekgül, M. Alper, H. Kockar, *J. Magn. Magn. Mater.* **421**, 472 (2017).

[33] B.G. Tóth, L. Péter, L. Pogány, Á. Révész, I. Bakonyi, *J. Electrochem. Soc.* **161**, D154 (2014).

[34] D. Zalka, L. Péter, M. El-Tahawy, J. Gubicza, G. Molnár, I. Bakonyi, *J. Electrochem. Soc.* **166**, D923 (2020).

[35] A. Tekgül, T. Şahin, H. Köçkar, M. Alper, *Optoelectron. Adv. Mat.* **14**, 189 (2020).

[36] X. Cheng, D. Cao, J. Du, L. Pan, H. Feng, Z. Zhu, J. Wei, J. Wang, Q. Liu, *J. Electrochem. Soc.* **164**, D154 (2017).

[37] T. Sahin, H. Kockar, M. Alper, *J. Magn. Magn. Mater.* **373**, 128 (2015).

[38] D. Grujicic, B. Pesic, *Electrochim. Acta* **47**, 2901 (2002).

[39] J. Ning, G. Xiao, L. Wang, B. Zou, B. Liu, G. Zou, *Nanoscale* **3**, 741 (2011).

[40] F. Břdker, M.F. Hansen, C.B. Koch, K. Lefmann, S. Mřrup, *Phys. Rev. B* **61**, 6826 (2000).

[41] L. Zhang, D. Xue, C. Gao, *J. Magn. Magn. Mater.* **267**, 111 (2003).

[42] M. Ştefănescu, T. Dippong, M. Stoia, O. Ştefănescu, *J. Therm. Anal. Calorim.* **94**, 389 (2008).